Improving ageing kinetics and precipitation hardening in an Al-Mg-Si alloy by minor Cd addition

Feng Qian[a], Eva A. Mørtsell[a], Calin D. Marioara[b], Sigmund J. Andersen[b], Yanjun Li[a,*]

[a] Department of Materials Science and Engineering, Norwegian University of Science and Technology, 7491, Trondheim, Norway

[b] SINTEF Materials and Nanotechnology, 7465, Trondheim, Norway

*Corresponding author. E-mail: yanjun.li@ntnu.no

Abstract

This study reports significant improvements in both the age hardening kinetics and peak hardness of an Al-Mg-Si alloy by microalloying with 0.06 at.% Cd. A detailed high-angle annular dark-field scanning transmission electron microscopy study shows that most of the needle-shaped hardening precipitates β'' (~82%) formed in the Cd-containing alloy are attached to or around Cd-rich precipitates, indicating that the Cd-rich precipitates can act as effective nucleation sites for needle-shaped precipitates, and therefore substantially increase the number density and decrease the size of needle-shaped precipitates. It also shows that most of the β'' precipitates in the Cd-containing alloy have a disordered structure, even at the peak-aged state. Additionally, Cu and/or Cd atoms are found to be incorporated into β'' and some precipitates with Q'/C-like triangular sub-units are formed, which are very rare in Al-Mg-Si alloys with a trace Cu content of 0.01 wt.%.

Keywords: Precipitates; Heterogeneous nucleation; Cd addition; Al-Mg-Si alloys; High-angle annular dark-field scanning transmission electron microscopy (HAADF-STEM)

As heat-treatable alloys, the 6xxx Al-Mg-Si alloys are featured by a significant increase in strength upon artificial ageing due to the formation of a high number density of nano-sized, (semi-)coherent, metastable precipitates (mainly β'' and Guinier-Preston (GP) zones [1,2]). Over the past decades, great efforts have been made to further improve the mechanical properties of Al-Mg-Si alloys. Modifications of the heat treatment, such as pre-ageing [3] and interrupted quenching [4], have proved to suppress the detrimental effect of natural ageing on artificial age hardening. T6I6 treatment (a T6 treatment interrupted by ageing at 25-65 °C before resuming to T6) was reported to enhance the age hardening response [5]. Optimisation of the alloying composition by increasing Si/Mg ratios also brought about an increase of hardness and a slower overageing response [6]. In terms of alloying additions, Cu [7–11], Ge [12], Ag [7], Zn [13] and Li [14] have shown to accelerate hardening kinetics and/or increase the peak strength. Among all the reported alloying additions, Cu is considered to be the best candidate for increasing the strength of Al-Mg-Si alloys. It was reported that an addition of 0.75 wt.% Cu could increase the hardness by up to 20 HV in the under-aged state and give about 6 HV higher peak hardness of AA6xxx alloy [10]. However, a Cu content higher than 0.1 wt.% in Al alloys can result in a severe reduction in corrosion resistance [15–17].

It has been demonstrated that the enhanced age hardening response of Al-Mg-Si alloys by microalloying with various elements is closely related to the modified precipitation sequence [9,12–14,18–20]. For example, Cu can suppress the precipitation of β'' and facilitate the formation of Cu-containing precipitates (e.g. Q', C and L [1]) [9,18]. Ge atoms were reported to substitute some of the Si atoms in β'' due to the similar electronic properties between Ge and Si [12,19]. Li preferentially occupies Mg3 sites in the β'' structure [14]. Zn shows a weaker preference for certain atomic sites, but a partial occupancy on Si3/Al sites was proposed [13,20]. Ag atoms are often observed at the incoherent precipitate/matrix interfaces or incorporated into β' precipitates by replacing certain Si atomic columns [21,22]. Recently, a new Q'/C-like local

configuration containing Ag at the Cu sites was discovered [19]. In addition, with the alloying additions, precipitates with disordered structures will become more common [13,19,23].

Additions of the impurity elements Cd, In and Sn have been reported to significantly increase the strength of Al-Cu alloys due to the refined dispersion of *θ'* [24–28]. Recently, it was found that a trace amount of Sn is also favourable for the Al-Mg-Si alloys by inhibiting natural ageing and therefore minimizing its detrimental effect on artificial age hardening, but no further increase of hardness was reported [29]. In this study, we demonstrate that a minor addition of 0.24 wt.% (0.06 at.%) Cd greatly accelerates the age-hardening kinetics of an Al-Mg-Si alloy and gives rise to a significant increase of peak hardness. Based on a careful observation of the precipitates using high-angle annular dark-field scanning transmission electron microscopy (HAADF-STEM), the underlying mechanism has been proposed.

Two Al-Mg-Si alloys were prepared by melting and casting into a copper mould with a dimension of 100 × 70 × 30 mm^3. For the Cd-containing Al-Mg-Si alloy, the Al-Cd master alloy was added at ~750 °C into the alloy melt. The alloy compositions are given in Table 1. Subsequently, the two as-cast alloys were solution heat-treated in an air-circulating furnace at 540 °C for 4 h and immediately quenched into water. After a room-temperature storage for 1 h, artificial ageing heat treatment was conducted in an oil bath at 185 °C for a range of times up to 24 h. Vickers hardness was measured using a 5 kg applied load and a dwell time of 15 s. Each data point was based on an average of at least eight measurements. Thin foils for transmission electron microscopy (TEM) study were made by a Struers Tenupol-5 twin-jet electropolisher operated at ~20 V, using a solution of 1/3 HNO_3 in methanol at ~ -28 °C. A JEOL 2100 operated at 200 kV was utilized for bright-field TEM observations and the quantification of precipitates (details of the methodology are given in Ref. [6,30]). All the images were taken along a $[001]_{Al}$ zone axis. HAADF-STEM micrographs were recorded by using a double aberration-corrected (image and probe Cs) cold-FEG JEOL ARM-200F

operated at 80 and 200 kV, respectively. The accelerating voltage of 80 kV was used for acquiring energy-dispersive X-ray spectroscopy (EDS) maps to reduce the radiation damage.

Figure 1 shows the hardness evolution of the two alloys as a function of ageing time at 185 °C. The Cd-containing alloy shows higher hardness for all ageing times and exhibits a much faster hardening kinetics than the Cd-free alloy. Prior to ageing, the hardnesses of both alloys are about 46 HV. After 30 min ageing, the hardness of the Cd-containing alloy has already doubled to 92 HV, while that of the Cd-free alloy is only 74 HV. Both alloys achieve peak hardnesses after ageing for 360 min, but the Cd-containing alloy has a wider hardness plateau. In contrast to the Cd-free alloy which gradually increases to the peak hardness, the Cd-containing alloy has already reached a hardness of 120 HV after 120 min ageing, which is very close to the peak hardness. Moreover, the peak hardness of the Cd-containing alloy is 6 HV higher than that of the Cd-free alloy.

Figure 2 shows bright-field TEM images of the Cd-free and Cd-containing alloys aged at 185 °C for different durations (30 and 360 min). For the purpose of comparison, the presented images in Figure 2 were taken at regions with similar sample thicknesses of 60~70 nm. After ageing for 30 min, black dots which correspond to precipitates can be seen in both alloys (Figure 2(a) and (b)). In the Cd-free alloy, the needle-shaped contrasts can be readily observed (Figure 2(a)), meaning needle-shaped β'' precipitates have formed and grown. In the Cd-containing alloy, the number density of precipitates is much higher, and most of the needle-shaped contrasts are shorter and blurred (Figure 2(b)). By assuming all the black dots are the cross-sections of needle-shaped precipitates in the viewing direction, the number density of precipitates in the Cd-containing alloy was estimated as 6.1×10^{23} m^{-3}, while that in the Cd-free alloy is 3.6×10^{22} m^{-3}. After 360 min ageing (peak-aged state), evident increases in the lengths and cross-sections of needle-shaped precipitates can be seen in the Cd-free alloy (Figure 2(c)). In the Cd-containing alloy, the needle-shaped contrasts become clearer, but their

lengths are still much shorter than the Cd-free alloy (Figure 2(d)). The quantified parameters of the precipitates in the two alloys aged for 360 min including cross-sections, needle lengths, number densities and volume fractions are given in Table 2. The number density of precipitates in the Cd-containing alloy is 2.6×10^{23} m^{-3}, which is six times greater than in the Cd-free alloy.

Figure 3 shows representative HAADF-STEM micrographs illustrating the cross-sections of precipitates in the Cd-containing alloy aged at 185 °C for 30 min. As shown in Figure 3(a), ultrafine nanoprecipitates with an average size of ~1.5 nm (marked by white arrows) have formed in the Al matrix. They have a near-circular shape and show a higher Z contrast than the Al matrix. The EDS analysis (not given here) shows that the precipitates are enriched with Cd, which is consistent with its relatively high Z contrast (Z_{Cd} = 48, Z_{Al} = 13, Z_{Mg} = 12, Z_{Si} = 14, Z_{Cu} = 29). Figure 3(b) represents the enlarged micrograph of one precipitate in Figure 3(a), in which the Cd-rich precipitate exhibits a much higher contrast (circled in green) than the Al matrix. A closer observation reveals that the Cd-rich precipitate is surrounded by another phase with a distinct structure. This phase is coherent with the Al matrix but with a slight lattice distortion, which gives rise to local configurations (indicated by yellow dashed circles) similar to the characteristic “eye” unit [31] (also referred to as “low density cylinder” (LDC) [32]) in the cross-section of needle-shaped β'' precipitate. However, the Z contrasts of the central sites in the eye-like units in Figure 3(b) are as high as (in some cases even higher than) that of the Al matrix, which is not consistent with the expected low Z contrast of Mg in the centre of the“eye” unit in β''. Therefore, this surrounding phase is more likely to be GP zones with the central sites of eye-like units being occupied by Al [31,33] or Si [34]. Of course, the possibility of partial Cu [35] or Cd occupation cannot be excluded. Figure 3(c) illustrates another Cd-rich precipitate marked by a green circle. It can be clearly seen that the atoms with bright contrast occupy Al fcc lattice positions, indicating that this Cd-rich precipitate is coherent with the α-

Al matrix. Around the Cd-rich precipitate, several eye-like units (marked by yellow dashed circles) are also observed.

Figure 4(a) shows the HAADF-STEM micrograph of precipitates in the Cd-containing alloy aged at 185 °C for 360 min. Cd-rich precipitates can still be observed (indicated by white arrows), but the sizes are slightly larger than those formed after 30 min ageing. Many needle-shaped precipitates (longitudinal sections indicated by orange ellipses and cross-sections by orange squares) are found to be associated with these Cd-rich precipitates. Figure 4(b) presents the enlarged micrograph of a typical "composite" precipitate in Figure 4(a), and the corresponding EDS maps are shown in Figure 4(c). Around the Cd-rich precipitate (circled in green in Figure 4(b)), several "eye" units can be clearly seen. However, no complete β'' unit cell can be identified, which means that the precipitate forming around the Cd-rich precipitate is a disordered β'' phase. It is also interesting to see that several columns show relatively high Z contrast (marked in a red dashed circle) within this precipitate. Although the EDS maps in Figure 4(c) do not show a clear elemental enrichment associated with these columns due to the resolution limit, it is speculated that Cd and/or Cu atoms have entered the precipitate and partially occupied these columns. To the best of authors' knowledge, the incorporation of Cd in β'' has never been reported before. The substitution of Cu atoms in β'' has been reported in Al-Mg-Si-Cu alloys with Cu contents higher than 0.5 wt.% [18,35]. However, the Cu content of the Cd-containing alloy in this study is rather low (0.01 wt.%), therefore, the precise crystal structure of this precipitate needs to be further investigated.

Figure 4(d) shows the atomistic structure of another type of "composite" precipitate, which is less frequently observed. The Cd-rich precipitate (in a green box) has a rectangular shape in the $[001]_{Al}$ projection and seems to have a periodic ordering on the lattice of Al matrix, which is different from the one shown in Figure 3(c). For the precipitate attached to it, Q'/C-like triangular sub-units (a sub-unit consisting of one Cu atom surrounded by three Mg atoms and

three Si atoms, as indicated by red dashed circles [18]) can be observed. The formation of Q'/C-like triangular sub-unit has never been reported in 6xxx alloys with such a low Cu content. However, there is also a possibility of the central Cu sites being replaced by Cd atoms. Further experimental and theoretical works are needed to address this issue.

The precipitation behaviours of the two alloys during ageing at 185 °C revealed by TEM (Figure 2-4) are well consistent with the age hardening response shown in Figure 1. The accelerated ageing kinetics and increased peak hardness of the Cd-containing alloy should be attributed to the enhanced nucleation of precipitates. According to the HAADF-STEM analyses on the Cd-containing alloy aged for 30 min (Figure 3), the high number density of precipitates (visualized as black dots in Figure 2(b)) consist mainly of Cd-rich precipitates and a small fraction of individual needle-shaped precipitates, and moreover, many Cd-rich precipitates are associated with needle-shaped precipitates. Based on the statistical analysis, the number density of the needle-shaped precipitates in the Cd-containing alloy aged for 30 min is corrected to be 2.3×10^{23} m^{-3} which is still much higher than that in the Cd-free alloy. It should be highlighted that the majority (~80%) of these needle-shaped precipitates are associated with Cd-rich precipitates.

Previously, Cd-rich precipitates formed in Al alloys were identified as the equilibrium hcp Cd phase or intermediate hcp Cd' phase with reduced lattice parameters [36,37]. A recent work on an AA3003 alloy microalloyed with Cd reported that most of the ultrafine Cd-rich precipitates formed during heating at 200-300 °C seem to have the same crystal structure and a similar lattice constant as the Al matrix, which is consistent with some of the Cd-rich precipitates observed in this study (Figure 3(c) and Figure 4(d)). For those Cd-rich precipitates with a more complicated structure (Figure 3(b)), a further investigation is required to determine its crystal structure.

In terms of the precipitation kinetics, the diffusion rate of Cd in Al is 7.1×10^{-15} cm^2/s at 185 °C, which is higher than those of Mg (2.7×10^{-15} cm^2/s) and Si (5.4×10^{-15} cm^2/s). It is proposed that the faster diffusion rate of Cd leads to the precipitation of Cd-rich precipitates prior to β" precipitates. Therefore, it is highly likely that the Cd-rich precipitates formed in the very early stage of artificial ageing act as heterogeneous nucleation sites for needle-shaped precipitates, which consequently results in a refined precipitate microstructure in the Cd-containing alloy.

More interestingly, it is found that the Cd addition in the Al-Mg-Si alloy has significantly modified the crystal structure of needle-shaped precipitates. Even after 360 min ageing, the complete unit cell of β'' cannot be observed in any cross-sections of needle-shaped precipitates in the Cd-containing alloy, which is completely different from the typical precipitate structure observed in conventional Al-Mg-Si(-Cu) alloys at the peak-aged state. In addition, Cu and/or Cd atoms are found to be incorporated into β'' precipitates by substituting certain columns (Figure 4(b)). A small fraction of precipitates with Q'/C-like triangular sub-units have also been found in the Cd-containing alloy with a Cu content as low as 0.01 wt.% (Figure 4(d)).

A very recent work reported that Sn has a similar effect as Cd shown in this work on refining the precipitate microstructure of Al-Mg-Si alloys aged at 250 °C [38]. However, no Sn precipitate formed during ageing. Instead, Sn atoms were found to preferentially occupy the Si sites of the β' phase and this β' phase is proposed to act as a heterogeneous nucleus for β''. This mechanism by which Sn prompts the β'' nucleation is different from that of Cd reported in this work.

It should be noted that Cd is a poisonous element, which is not likely to be used in commercial alloys. However, the highlight of our work is to propose an effective method for promoting the heterogeneous nucleation of strengthening precipitates in Al-Mg-Si alloys. Searching for non-

toxic elements with similar strengthening mechanism in Al-Mg-Si alloys will be the emphasis of the future work.

In summary, we have shown that a minor addition of Cd (0.06 at.%) in an Al-Mg-Si alloy can lead to a much more rapid hardening response as well as a significant increase in peak hardness due to an enhanced precipitation. HAADF-STEM analyses indicate that the densely dispersed, nano-sized Cd-rich precipitates formed in the early stage of artificial ageing act as effective nucleation sites for the needle-shaped hardening precipitates. Closer HAADF-STEM observations reveal that most of β'' show a disordered structure in the Cd-containing alloy. Besides, Cu and/or Cd atoms are found to be incorporated into β'', and some precipitates with Q'/C-like triangular sub-units have formed.

Acknowledgements

The authors are grateful for the Norwegian Centre of Transmission Electron Microscopy (NORTEM) at NTNU, where the TEM work has been carried out.

References

[1] C. Ravi, C. Wolverton, First-principles study of crystal structure and stability of Al–Mg–Si–(Cu) precipitates, Acta Materialia. 52 (2004) 4213–4227. doi:https://doi.org/10.1016/j.actamat.2004.05.037.

[2] P.H. Ninive, A. Strandlie, S. Gulbrandsen-Dahl, W. Lefebvre, C.D. Marioara, S.J. Andersen, et al., Detailed atomistic insight into the β″ phase in Al–Mg–Si alloys, Acta Materialia. 69 (2014) 126–134. doi:10.1016/j.actamat.2014.01.052.

[3] J.D. Bryant, The effects of preaging treatments on aging kinetics and mechanical properties in AA6111 aluminum autobody sheet, Metallurgical and Materials Transactions A. 30 (1999) 1999–2006. doi:10.1007/s11661-999-0010-3.

[4] S. Pogatscher, H. Antrekowitsch, H. Leitner, D. Pöschmann, Z.L. Zhang, P.J. Uggowitzer, Influence of interrupted quenching on artificial aging of Al–Mg–Si alloys, Acta Materialia. 60 (2012) 4496–4505. doi:https://doi.org/10.1016/j.actamat.2012.04.026.

[5] J. Buha, R.N. Lumley, A.G. Crosky, K. Hono, Secondary precipitation in an Al–Mg–Si–Cu alloy, Acta Materialia. 55 (2007) 3015–3024. doi:https://doi.org/10.1016/j.actamat.2007.01.006.

[6] C.D. Marioara, S.J. Andersen, H.W. Zandbergen, R. Holmestad, The influence of alloy composition on precipitates of the Al-Mg-Si system, Metallurgical and Materials Transactions A. 36 (2005) 691–702. doi:10.1007/s11661-005-0185-1.

[7] J. Kim, C. Daniel Marioara, R. Holmestad, E. Kobayashi, T. Sato, Effects of Cu and Ag additions on age-hardening behavior during multi-step aging in Al-Mg-Si alloys, Materials Science and Engineering: A. 560 (2013) 154–162. doi:https://doi.org/10.1016/j.msea.2012.09.051.

[8] C.D. Marioara, S.J. Andersen, T.N. Stene, H. Hasting, J. Walmsley, A.T.J. Van Helvoort, et al., The effect of Cu on precipitation in Al–Mg–Si alloys, Philosophical Magazine. 87 (2007) 3385–3413. doi:10.1080/14786430701287377.

[9] D.J. Chakrabarti, D.E. Laughlin, Phase relations and precipitation in Al–Mg–Si alloys with Cu additions, Progress in Materials Science. 49 (2004) 389–410. doi:https://doi.org/10.1016/S0079-6425(03)00031-8.

[10] M.W. Zandbergen, A. Cerezo, G.D.W. Smith, Study of precipitation in Al–Mg–Si Alloys by atom probe tomography II. Influence of Cu additions, Acta Materialia. 101 (2015) 149–158. doi:10.1016/j.actamat.2015.08.018.

[11] W.F. Miao, D.E. Laughlin, Effects of Cu content and preaging on precipitation characteristics in aluminum alloy 6022, Metallurgical and Materials Transactions A. 31 (2000) 361–371. doi:10.1007/s11661-000-0272-2.

[12] E.A. Mørtsell, C.D. Marioara, S.J. Andersen, J. Røyset, O. Reiso, R. Holmestad, Effects of Germanium, Copper, and Silver Substitutions on Hardness and Microstructure in Lean Al-Mg-Si Alloys, Metallurgical and Materials Transactions A. 46 (2015) 4369–4379. doi:10.1007/s11661-015-3039-5.

[13] T. Saito, S. Wenner, E. Osmundsen, C.D. Marioara, S.J. Andersen, J. Røyset, et al., The effect of Zn on precipitation in Al–Mg–Si alloys, Philosophical Magazine. 94 (2014)

2410–2425. doi:10.1080/14786435.2014.913819.

[14] E.A. Mørtsell, C.D. Marioara, S.J. Andersen, I.G. Ringdalen, J. Friis, S. Wenner, et al., The effects and behaviour of Li and Cu alloying agents in lean Al-Mg-Si alloys, Journal of Alloys and Compounds. 699 (2017) 235–242. doi:https://doi.org/10.1016/j.jallcom.2016.12.273.

[15] W.J. Liang, P.A. Rometsch, L.F. Cao, N. Birbilis, General aspects related to the corrosion of 6xxx series aluminium alloys: Exploring the influence of Mg/Si ratio and Cu, Corrosion Science. 76 (2013) 119–128. doi:https://doi.org/10.1016/j.corsci.2013.06.035.

[16] S.K. Kairy, P.A. Rometsch, K. Diao, J.F. Nie, C.H.J. Davies, N. Birbilis, Exploring the electrochemistry of 6xxx series aluminium alloys as a function of Si to Mg ratio, Cu content, ageing conditions and microstructure, Electrochimica Acta. 190 (2016) 92–103. doi:https://doi.org/10.1016/j.electacta.2015.12.098.

[17] G. Svenningsen, M.H. Larsen, J.C. Walmsley, J.H. Nordlien, K. Nisancioglu, Effect of artificial aging on intergranular corrosion of extruded AlMgSi alloy with small Cu content, Corrosion Science. 48 (2006) 1528–1543. doi:https://doi.org/10.1016/j.corsci.2005.05.045.

[18] L. Ding, Z. Jia, J. Nie, Y. Weng, L. Cao, H. Chen, et al., The structural and compositional evolution of precipitates in Al-Mg-Si-Cu alloy, Acta Materialia. 145 (2018) 437–450. doi:https://doi.org/10.1016/j.actamat.2017.12.036.

[19] E.A. Mørtsell, S.J. Andersen, J. Friis, C.D. Marioara, R. Holmestad, Atomistic details of precipitates in lean Al–Mg–Si alloys with trace additions of Ag and Ge studied by HAADF-STEM and DFT, Philosophical Magazine. 97 (2017) 851–866. doi:10.1080/14786435.2017.1281461.

[20] T. Saito, F.J.H. Ehlers, W. Lefebvre, D. Hernandez-Maldonado, R. Bjørge, C.D. Marioara, et al., HAADF-STEM and DFT investigations of the Zn-containing β″ phase in Al–Mg–Si alloys, Acta Materialia. 78 (2014) 245–253. doi:10.1016/j.actamat.2014.06.055.

[21] C.D. Marioara, J. Nakamura, K. Matsuda, S.J. Andersen, R. Holmestad, T. Sato, et al., HAADF-STEM study of β ′-type precipitates in an over-aged Al–Mg–Si–Ag alloy, Philosophical Magazine. 92 (2012) 1149–1158. doi:10.1080/14786435.2011.642319.

[22] S. Wenner, C.D. Marioara, Q.M. Ramasse, D.-M. Kepaptsoglou, F.S. Hage, R. Holmestad, Atomic-resolution electron energy loss studies of precipitates in an Al–Mg–Si–Cu–Ag alloy, Scripta Materialia. 74 (2014) 92–95. doi:10.1016/j.scriptamat.2013.11.007.

[23] S. Wenner, C.D. Marioara, S.J. Andersen, R. Holmestad, Effect of room temperature storage time on precipitation in Al–Mg–Si(–Cu) alloys with different Mg/Si ratios, International Journal of Materials Research. 103 (2012) 948–954. doi:10.3139/146.110795.

[24] H.K. Hardy, The ageing characteristics of ternary aluminium-copper alloys with cadmium, indium, or tin, Journal of the Institute of Metals. 80 (1951) 483.

[25] B. Noble, Theta-prime precipitation in aluminium-copper-cadmium alloys, Acta Metallurgica. 16 (1968) 393–401. doi:10.1016/0001-6160(68)90026-6.

[26] S.P. Ringer, K. Hono, T. Sakurai, The effect of trace additions of sn on precipitation in Al-Cu alloys: An atom probe field ion microscopy study, Metallurgical and Materials Transactions A. 26 (1995) 2207–2217. doi:10.1007/BF02671236.

[27] J.M. Silcock, H.M. Flower, Comments on a comparison of early and recent work on the effect of trace additions of Cd, In, or Sn on nucleation and growth of θ′ in Al–Cu alloys, Scripta Materialia. 46 (2002) 389–394. doi:10.1016/S1359-6462(02)00003-9.

[28] L. Bourgeois, C. Dwyer, M. Weyland, J.-F. Nie, B.C. Muddle, The magic thicknesses of θ′ precipitates in Sn-microalloyed Al–Cu, Acta Materialia. 60 (2012) 633–644. doi:10.1016/j.actamat.2011.10.015.

[29] S. Pogatscher, H. Antrekowitsch, M. Werinos, F. Moszner, S.S.A. Gerstl, M.F. Francis, et al., Diffusion on Demand to Control Precipitation Aging: Application to Al-Mg-Si Alloys, Physical Review Letters. 112 (2014) 225701. doi:10.1103/PhysRevLett.112.225701.

[30] S.J. Andersen, Quantification of the Mg2Si β″ and β′ phases in AlMgSi alloys by transmission electron microscopy, Metallurgical and Materials Transactions A. 26 (1995) 1931–1937. doi:10.1007/BF02670664.

[31] C.D. Marioara, S.J. Andersen, J. Jansen, H.W. Zandbergen, Atomic model for GP-zones in a 6082 Al–Mg–Si system, Acta Materialia. 49 (2001) 321–328. doi:10.1016/S1359-6454(00)00302-5.

[32] M.A. van Huis, J.H. Chen, M.H.F. Sluiter, H.W. Zandbergen, Phase stability and structural features of matrix-embedded hardening precipitates in Al–Mg–Si alloys in the early stages of evolution, Acta Materialia. 55 (2007) 2183–2199. doi:https://doi.org/10.1016/j.actamat.2006.11.019.

[33] S. Wenner, L. Jones, C.D. Marioara, R. Holmestad, Atomic-resolution chemical mapping of ordered precipitates in Al alloys using energy-dispersive X-ray spectroscopy, Micron. 96 (2017) 103–111. doi:https://doi.org/10.1016/j.micron.2017.02.007.

[34] M.A. van Huis, J.H. Chen, H.W. Zandbergen, M.H.F. Sluiter, Phase stability and structural relations of nanometer-sized, matrix-embedded precipitate phases in Al–Mg–Si alloys in the late stages of evolution, Acta Materialia. 54 (2006) 2945–2955. doi:https://doi.org/10.1016/j.actamat.2006.02.034.

[35] K. Li, A. Béché, M. Song, G. Sha, X. Lu, K. Zhang, et al., Atomistic structure of Cu-containing β″ precipitates in an Al–Mg–Si–Cu alloy, Scripta Materialia. 75 (2014) 86–89. doi:https://doi.org/10.1016/j.scriptamat.2013.11.030.

[36] J.M. Silcock, T.J. Heal, H.K. Hardy, The structural ageing characteristics of ternary aluminium-copper alloys wih cadimium, indium, or tin, Journal of the Institute of Metals. 84 (1955) 23.

[37] J.M. Silcock, Intermediate precipitates in aged binary alloys of aluminium with cadmium, indium and tin, Journal of the Institute of Metals. 84 (1955) 19.

[38] C. Liu, P. Ma, L. Zhan, M. Huang, J. Li, Solute Sn-induced formation of composite β′/β″ precipitates in Al-Mg-Si alloy, Scripta Materialia. 155 (2018) 68–72. doi:https://doi.org/10.1016/j.scriptamat.2018.06.028.

Tables

Table 1 Chemical compositions (wt.%) of the experimental materials.

Alloy	Mn	Fe	Si	Mg	Cd	Cu	Al
Cd-free	0.50	0.20	1.12	0.55	-	0.01	bal.
Cd-containing	0.52	0.21	1.06	0.50	0.24	0.01	bal.

Table 2 Measured average cross-sections, needle lengths, number densities and volume fractions of precipitates in the two alloys after artificial ageing at 185 °C for 360 min.

Alloy	Cross-section (nm^2)	Needle length (nm)	Number density ($\times 10^{22}$ m^{-3})	Volume fraction (%)
Cd-free	8.5 ± 4.7	44.5 ± 19.5	3.6 ± 0.3	1.4
Cd-containing	4.2 ± 1.9	14.5 ± 5.8	26.2 ± 3.7	1.6

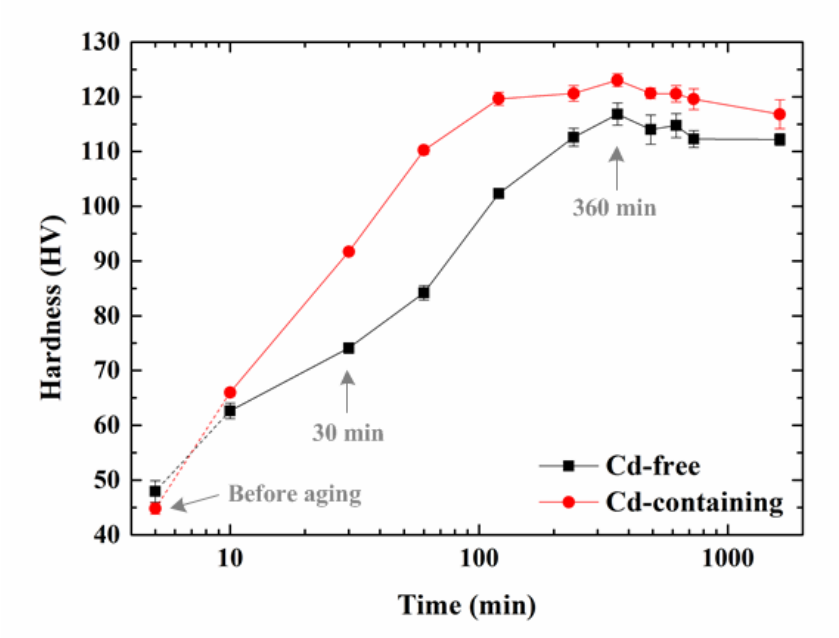

Figure 1 Hardness evolution of the Cd-free and Cd-containing alloys during ageing at 185 °C.

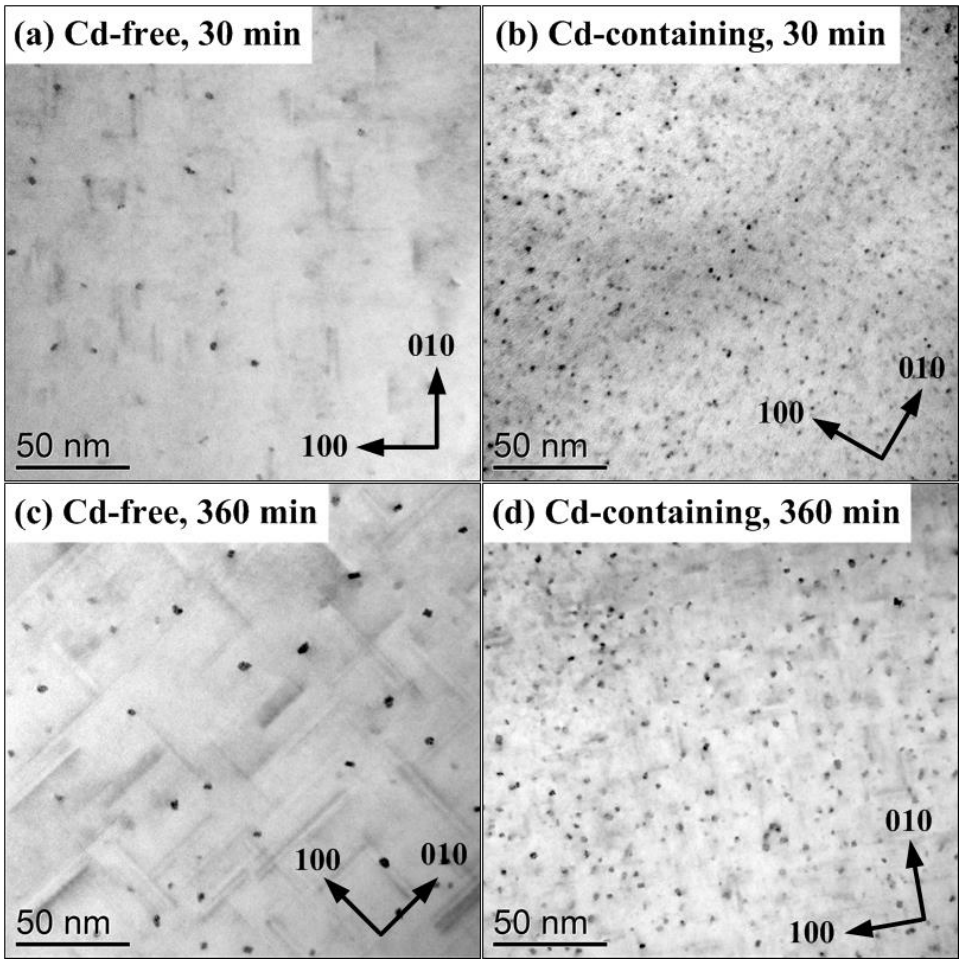

Figure 2 Bright-field TEM micrographs of the Cd-free and Cd-containing alloys aged at 185 °C for 30 min and 360 min. The sample thicknesses of the presented regions in (a)-(d) are 70 nm, 64 nm, 60 nm and 67 nm, respectively.

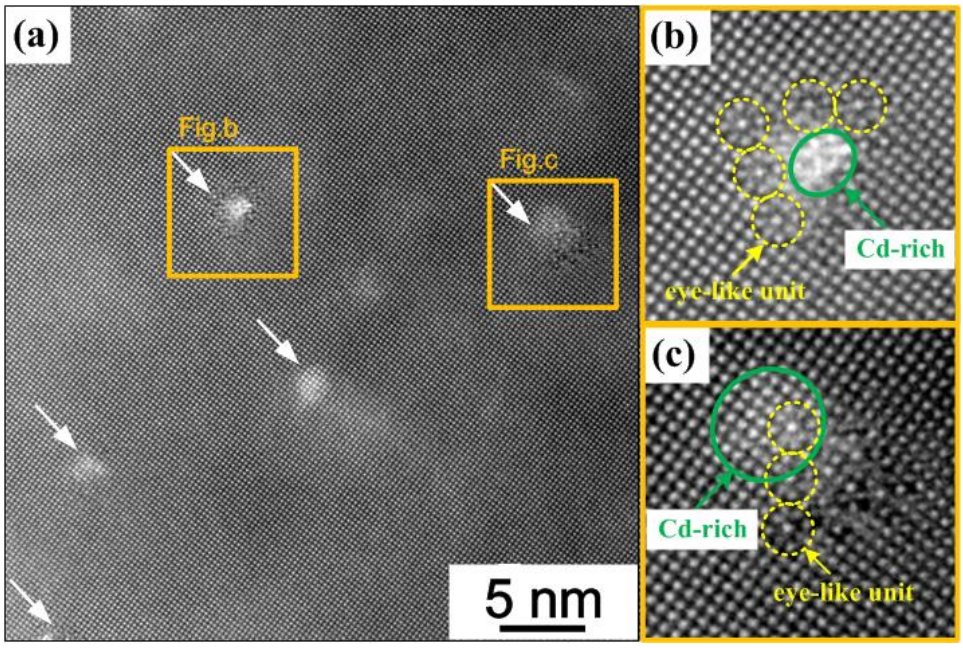

Figure 3 (a) HAADF-STEM micrograph of the early-stage precipitates in the Cd-containing alloy aged at 185 °C for 30 min. (b) and (c) show the enlarged areas indicated in (a). For interpretation of the references to colour in this figure legend, the reader is referred to the web version of this article.

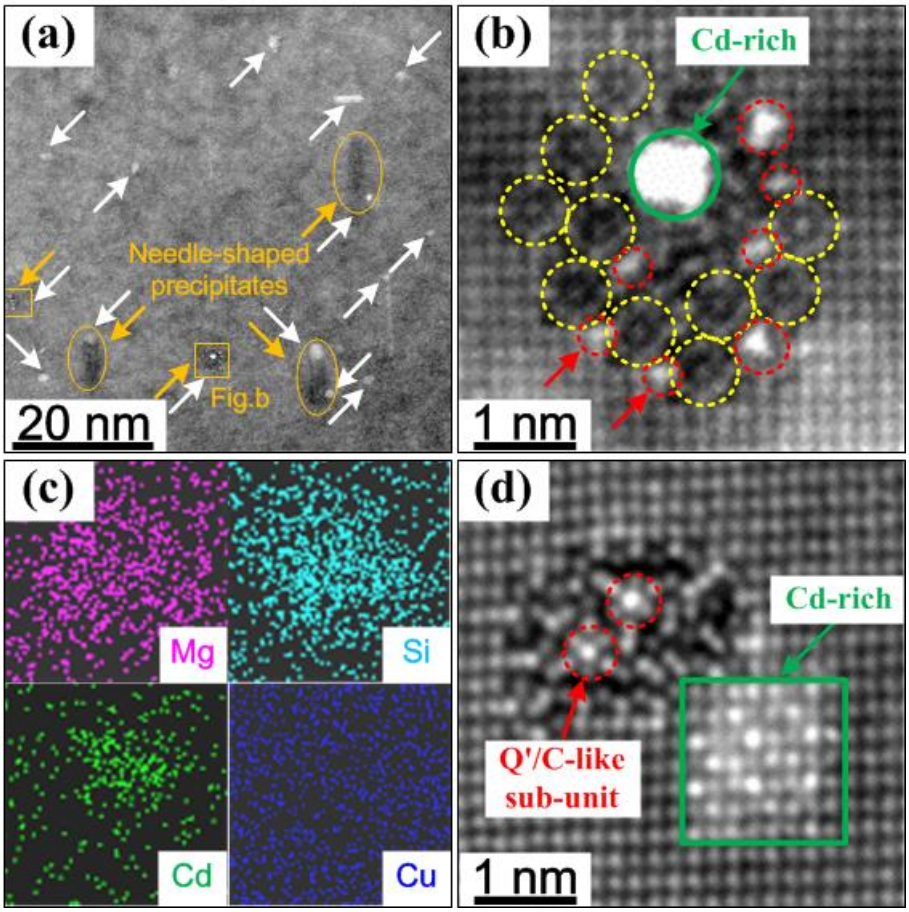

Figure 4 (a) HAADF-STEM micrograph of precipitates in the Cd-containing alloy aged at 185 °C for 360 min. (b) Enlarged HAADF-STEM micrograph of one typical "composite" precipitate and (c) the corresponding EDS elemental maps. (d) HAADF-STEM micrograph of another "composite" precipitate. For interpretation of the references to colour in this figure legend, the reader is referred to the web version of this article.